Validated analysis of modulated signals:
from de Prony to Padé and beyond

Annie Cuyt[a,c], Yuan Hou[a], Wen-shin Lee[b,*]

[a]*Computational & Engineering Mathematics (CEMath), Universiteit Antwerpen*
Middelheimlaan 1, B-2020 Antwerpen, Belgium
[b]*Computing Science and Mathematics, University of Stirling*
Stirling FK9 4LA, Scotland, UK
[c]*College of Mathematics and Statistics, Shenzhen University*
Shenzhen, Guangdong 518060, China

Remembering Luc Wuytack who introduced me to the concept of Padé approximation

Annie Cuyt

Abstract

The spectral analysis of modulated signals has attracted quite some research, mainly because of the fact that Fourier methods are not particularly suitable. Among the challenges, we mention the separation of close components that differ significantly in magnitude, the limitation of the sampling duration, the probable ill-conditioning of certain structured matrices.

We show how a validated exponential analysis add-on, for use with any standard exponential analysis method, offers a lot of advantages in the context of these challenges. The add-on uses an alias-free decimation technique and essentially combines the basics of de Prony's method for exponential fitting with the theory of Padé approximation theory.

Keywords: Exponential analysis, modulation, validation, decimation, Prony polynomial, Padé approximant, Froissart doublet.

2010 MSC: 41A21, 42A15, 65D05, 65T40, 65Z05

---

*Corresponding author

Email addresses: `annie.cuyt@uantwerpen.be` (Annie Cuyt), `yuan.hou@uantwerpen.be` (Yuan Hou), `wen-shin.lee@stir.ac.uk` (Wen-shin Lee)

1. Introduction

When dealing with non-stationary signals, the widely used efficient and robust Fourier transform is not very useful. Its frequency resolution depends on the sampling duration and the latter is very limited when the signal is not stationary. Also the spectral leakage of the Fourier transform complicates the distinction of multiple components close to each other, especially if the components differ significantly in magnitude. Such situation often occurs in modulated signals.

To overcome these drawbacks, several other algorithms have been proposed, among which various wavelet-based transforms, neural network approaches, genetic algorithms, extensions of Kalman filtering, and methods based on de Prony's computational scheme. The latter methods are often confronted with possibly ill-conditioned Hankel matrices and are usually quite sensitive to noise. Also, distinguishing multiple components close to one another in a narrow frequency band remains difficult because of the necessity to work with large matrices. We propose a validated version of de Prony's method [1, 2] by combining it with results from Padé approximation theory [3, 4, 5], generalized eigenvalue algorithms [6], observations by the theoretical physicist Froissart [7, 8] and decimation as presented in [9, 10] to recondition and divide-and-conquer larger sized problems. We thus bring together mathematical research results from 4 different centuries, from the end of the 18-th century to the beginning of the 21-st century.

The basic steps used in recent versions of de Prony's method, when applied to non-modulated signals, are summarized in Section 2. In Section 3 we deal with various types of modulation and discuss how to adapt the method presented in Section 2. So far for the mathematics underlying modulation.

In Section 4 we summarize a recent validated implementation of de Prony's method for use with non-modulated signals. At the same time we develop the adaptations required to deal with modulated signals. The new results are illustrated in Section 5, on a number of practical examples from the scientific

2

literature.

2. Standard exponential analysis

Exponential analysis in signal processing is an inverse problem. Let the signal $f(t)$ be given by

$$f(t) = \sum_{j=1}^{n} \alpha_j \exp(\phi_j t), \qquad \alpha_j, \phi_j \in \mathbb{C}. \tag{1}$$

Already in 1795, de Prony [1] proved that the values of the coefficients $\alpha_j, j = 1, \ldots, n$ and the mutually distinct exponents $\phi_j, j = 1, \ldots, n$ can be recovered from a mere $2n$ equidistant samples if the sparsity n is known. Much later, the connection to Padé approximation was pointed out in [11] and the problem statement was reformulated as a structured generalized eigenvalue problem in [6]. For the sake of completeness we summarize these connections, at the same time indicating some practical aspects concerning the numerical computation of the unknowns $\phi_j, \alpha_j, j = 1, \ldots, n$. How n can be determined, is discussed further on. It is usually considered a hard problem, while an incorrect estimate of the sparsity greatly influences the computed results.

Let $\Im(\cdot)$ denote the imaginary part of a complex number. Sometimes the coefficients α_j are referred to as the complex amplitudes (the real amplitudes equal $|\alpha_j|$) and the ϕ_j as the complex frequencies (the real frequencies equal $\Im(\phi_j)$). In the following we choose a real $\Delta \neq 0$ such that $|\Im(\phi_j)| < \pi/|\Delta|$, in order to comply with [12, 13]. The value Δ denotes the sampling step in the equidistant sampling scheme

$$f_k := f(k\Delta) = \sum_{j=1}^{n} \alpha_j \exp(\phi_j k\Delta) = \sum_{j=1}^{n} \alpha_j \Phi_j^k, \qquad \Phi_j = \exp(\phi_j \Delta). \tag{2}$$

We start with the generalized eigenvalue reformulation of the exponential analysis problem. With the samples $f_k, k = 0, \ldots, 2n-1, \ldots$ we fill the Hankel matrices

$$H_n^{(m)} := \left(f_{m+i+j-2} \right)_{i,j=1}^{n} = \begin{pmatrix} f_m & f_{m+1} & \cdots & f_{m+n-1} \\ f_{m+1} & f_{m+2} & \cdots & f_{m+n} \\ \vdots & \vdots & \ddots & \vdots \\ f_{m+n-1} & f_{m+n} & \cdots & f_{m+2n-2} \end{pmatrix}, \qquad m \geq 0.$$

3

From the expression (2) for the samples f_k we immediately find that $H_n^{(m)}$ can be factored as

$$H_n^{(m)} = V_n D_\alpha D_\Phi^m V_n^T, \tag{3}$$

where V_n is the Vandermonde matrix

$$V_n = \left(\Phi_j^{i-1}\right)_{i,j=1}^n$$

and D_α and D_Φ are diagonal matrices respectively filled with the vectors $(\alpha_1, \ldots, \alpha_n)$ and $(\Phi_1, \ldots, \Phi_n)$ on the diagonal. So the $\Phi_j, j = 1, \ldots, n$ can be found as the generalized eigenvalues $\lambda_j, j = 1, \ldots, n$ of the problem [6]

$$H_n^{(1)} v_j = \lambda_j H_n^{(0)} v_j, \tag{4}$$

where the $v_j, j = 1, \ldots, n$ are the right generalized eigenvectors. From the generalized eigenvalues $\Phi_j = \exp(\phi_j \Delta)$ the complex values ϕ_j can be extracted uniquely because $|\Im(\phi_j)\Delta| < \pi$. After recovering the Φ_j, the α_j can be computed from the Vandermonde structured linear system

$$\sum_{j=1}^n \alpha_j \Phi_j^k = f_k, \qquad k = 0, \ldots, 2n - 1, \ldots \tag{5}$$

In a noisefree mathematical context, only n equations of (5) are linearly independent because of the relationship (4) between the Φ_j. How to reliably proceed in a noisy context is analyzed in great detail in [10].

Instead of filling Hankel matrices with the samples f_k, we can also construct a formal power series expansion

$$F(z) = \sum_{k=0}^\infty f_k z^k.$$

The series expansion $F(z)$ is related to the z-transform $Z(f)$ of the sequence $(f_k)_{k\in\mathbb{N}}$ by $Z(f) = F(1/z)$. Using the expression (2) for the f_k and under the assumption that the Φ_j are mutually distinct, it is not difficult to see that [11]

$$F(z) = \sum_{k=0}^\infty \left(\sum_{j=1}^n \alpha_j \Phi_j^k\right) z^k = \sum_{j=1}^n \alpha_j \left(\sum_{k=0}^\infty \Phi_j^k z^k\right) = \sum_{j=1}^n \frac{\alpha_j}{1 - \Phi_j z}. \tag{6}$$

So the function $F(z)$ is itself a rational function of degree $n-1$ in the numerator and n in the denominator. The consistency property of Padé approximants

4

guarantees that a rational function like $F(z)$ is reconstructed from its formal series expansion by its $[n-1/n]_F$ Padé approximant of degree $n-1$ in the numerator and n in the denominator, thereby needing only the series coefficients $f_0, \ldots, f_{2n-1}$. So we can also obtain the Φ_j from the Padé denominator

$$\prod_{j=1}^{n}(1 - \Phi_j z) = b_n z^n + \ldots + b_1 z + 1, \tag{7}$$

as inverses of the poles of $[n-1/n]_F$, and the α_j from the partial fraction decomposition of $[n-1/n]_F$ in (6). Let us reconnect to de Prony's original algorithm. The reverse of the Padé denominator, namely the polynomial

$$\prod_{j=1}^{n}(z - \Phi_j) = z^n + b_1 z^{n-1} + \ldots + b_n, \tag{8}$$

is called the Prony polynomial. Its coefficients are obtained from a Hankel structured system [2, pp. 378–382], which is a mere rewrite of the Toeplitz linear system that delivers the Padé denominator coefficients, namely

$$\begin{pmatrix} f_{n-1} & \cdots & f_0 \\ \vdots & \ddots & \vdots \\ f_{2n-2} & \cdots & f_{n-1} \end{pmatrix} \begin{pmatrix} b_1 \\ \vdots \\ b_n \end{pmatrix} = H_n^{(0)} \begin{pmatrix} b_n \\ \vdots \\ b_1 \end{pmatrix} = -\begin{pmatrix} f_n \\ \vdots \\ f_{2n-1} \end{pmatrix}. \tag{9}$$

Now what can be said about n? Merely using some known theorems, its value can be nailed down quite precisely, that is, again in an exact noisefree context. Let $|H_n^{(m)}|$ denote $\det H_n^{(m)}$. We read in [14] and [15] that on the one hand, for $N < n$ and $m \geq 0$, $|H_N^{(m)}|$ is only accidentally zero, depending on the value of Δ, while on the other hand, for $N > n$ and $m \geq 0$, $|H_N^{(m)}|$ is always zero, irrespective of the value of Δ. Most importantly, for $N = n, m \geq 0$ and mutually distinct Φ_j, $|H_n^{(m)}| \neq 0$. In order to inspect $|H_N^{(m)}|$ for $N > n$, additional samples up to f_{m+2N-2} need to be provided, in other words at least the additional sample f_{2n} (in case $m = 0$ and $N = n+1$). A nice discussion, based on algebraic arguments, is presented in [16].

In the case where the $f_k, k = 0, 1, 2, \ldots$ are perturbed with noise,

$$F(z) + \epsilon(z) = \sum_{k=0}^{\infty}(f_k + \epsilon_k)z^k,$$

we need to proceed differently to detect the sparsity n. The theorem of Nuttall-Pommerenke states that if $F(z)+\epsilon(z)$ is analytic throughout the complex plane, except for a countable number of poles [4] and essential singularities [5], then its sequence of Padé approximants $\{[\eta - 1/\eta]_F(z)\}_{\eta \in \mathbb{N}}$ of degree $\eta - 1$ over η converges to $F(z) + \epsilon(z)$ in measure on compact sets. This means that for sufficiently large η the measure of the set where the convergence is disrupted, so where $|F(z) + \epsilon(z) - [\eta - 1/\eta]_F(z)| \geq \tau$ for some given threshold τ, tends to zero as η tends to infinity.

In our case, pointwise convergence is disrupted by $\eta - n$ unwanted pole-zero combinations of the Padé approximants that are added to the n true poles and $n-1$ true zeros of $F(z)$, the pole and zero in the pair almost cancelling each other locally [17, 8]. These pole-zero combinations are also referred to as Froissart doublets. In practice, these Froissart doublets offer a way to separate the noise $\epsilon(z)$ from the underlying $F(z)$. Because of the Padé convergence theorem, the true poles can be identified as stable poles in successive $[\eta - 1/\eta]_F(z)$, while the noisy poles are distinguished by their instability. When increasing η we compute a larger set of poles, of which the noisy ones are moving around [18, 8] with every different realization of the noise $\epsilon(z)$. The true Φ_j are forming stable clusters while the ones related to noise are scattered.

This characteristic enables to develop a validated algorithm [10] for the identification of the unknown model parameters in (1). Decimation by a factor r of a sufficiently large number $N \geq 2n$ of samples f_k, allows to compute $\lfloor N/2r \rfloor = \eta > n$ generalized eigenvalues per decimated subset and inspect the stable poles and Froissart doublets of the $r \times \eta$ joint results. In a nutshell:

- the sparsity n equals the number of identified clusters of Φ_j,

- ideally each cluster contains (close to) r elements,

- $\Phi_1, \ldots, \Phi_n$ are the centers of gravity of these clusters,

- $\alpha_1, \ldots, \alpha_n$ satisfy the $N \times n$ Vandermonde system (5).

6

The details of the technique are recapped in Section 4.1, while an adaptation for certain modulated signals is given in Section 4.2.

3. Analysis of modulated signals

Exponential analysis might sound remote, but it touches our lives in many surprising ways, even if most people are unaware of just how important it is. For example, a substantial amount of effort in the field of signal processing is essentially dedicated to the analysis of multi-exponential functions of which the exponents ϕ_j are complex. The analysis of exponential functions whose exponents are very near each other is directly linked to super-resolution imaging. As for multi-exponential functions with real exponents ϕ_j, they are used to portray relaxation, chemical reactions, radioactivity, heat transfer, fluid dynamics.

Besides signals which follow an exponential model with constant ϕ_j and α_j, several applications rely on a signal model where the parameters are themselves time-dependent. In this section we treat signals with modulated amplitudes $\alpha_j(t)$ where the modulation can take different forms, in particular polynomial and trigonometric expressions for $\alpha_j(t)$, and we discuss some forms of frequency modulation. In Section 5 we list a number of engineering applications in which modulated signals appear naturally.

3.1. Polynomial amplitude modulation

Let the signal be given by

$$f(t) = \sum_{j=1}^{n} \left[\alpha_{j0} + \sum_{\ell=1}^{\mu_j-1} \alpha_{j\ell} \binom{\ell + t/\Delta}{\ell} \right] \exp(\phi_j t), \qquad \alpha_{j\ell}, \phi_j \in \mathbb{C}. \qquad (10)$$

As above, we sample (10) at the equidistant points $k\Delta$ to obtain $f_k, k = 0, 1, 2, \ldots$ Now

$$f_k := \sum_{j=1}^{n} \left[\sum_{\ell=0}^{\mu_j-1} \alpha_{j\ell} \binom{\ell + k}{\ell} \right] \Phi_j^k. \qquad (11)$$

It was proved in [19] that the function

$$F(z) = \sum_{k=0}^{\infty} f_k z^k = \sum_{j=1}^{n} \sum_{\ell=0}^{\mu_j-1} \frac{\alpha_{j\ell}}{(1 - \Phi_j z)^{\ell+1}}$$

7

is a rational function of degree $\mathfrak{n} - 1$ in the numerator and degree $\mathfrak{n}$ in the denominator where $\mathfrak{n} = \mu_1 + \cdots + \mu_n$ and hence can be reconstructed by the computation of the Padé approximant $[\mathfrak{n} - 1/\mathfrak{n}]_F$ from its series development. Clearly, modulation of the amplitudes increases the denominator degree of the Padé approximant. In the case of polynomial modulation, it does so by raising the multiplicity of the Padé pole $1/\Phi_j$ to μ_j, which is one more than the degree of the j-th polynomial amplitude.

Also, with modulation as in (10) or (13), the parameters $\phi_j, j = 1, \ldots, n$ are identified from (8) rather than (4). The reason is that in the case of multiple poles, factorization (3) of $H_n^{(m)}$, which leads to the generalized eigenvalue algorithm, does not hold. The Padé denominator (7) or its reverse, the Prony polynomial, can be computed using (9). With roots of higher multiplicity the Vandermonde system (5) needs to be replaced by a confluent version for the computation of the α_j. We come back on this issue in Section 4.2.

3.2. Trigonometric amplitude modulation

In several applications the amplitude is modulated periodically. Let the signal be given by

$$f(t) = \sum_{j=1}^{n} \left[\alpha_{j0} + \sum_{\ell=1}^{\mu_j-1} \alpha_{j\ell} \exp(\phi_{j\ell}t) \right] \exp(\phi_{j0}t), \qquad \alpha_{j\ell}, \phi_{j\ell} \in \mathbb{C}. \qquad (12)$$

Using the results of Section 2, it is easy to see that with

$$\Phi_{j\ell} = \exp(\phi_{j\ell}\Delta), \qquad j = 1, \ldots, n, , \qquad \ell = 0, \ldots, \mu_j - 1,$$

the exponential model (12) translates to the Padé approximation problem of denominator degree $\mathfrak{n} = \mu_1 + \cdots + \mu_n$ and numerator degree $\mathfrak{n} - 1$ of the rational function

$$F(z) = \sum_{k=0}^{\infty} f_k z^k = \sum_{j=1}^{n} \left[\frac{\alpha_{j0}}{1 - \Phi_{j0}z} + \sum_{\ell=1}^{\mu_j-1} \frac{\alpha_{j\ell}}{1 - \Phi_{j0}\Phi_{j\ell}z} \right].$$

Again modulation of the amplitude increases the denominator degree of the Padé approximant, from n to $\mu_1 + \cdots + \mu_n$, where for $1 \le j \le n$, $\mu_j - 1$ of these terms modulate the amplitude α_{j0}.

8

3.3. Related amplitude modulation

In [20, 21] several variations of exponential analysis are presented, using among others

- certain orthogonal polynomials,

- different trigonometric building functions,

- the sampling function sinc,

- the Gaussian distribution function.

Similar variations can be considered in the context of modulation. For instance, a sinc modulated amplitude, as in the signal

$$f(t) = \sum_{j=1}^{n} [\alpha_j + \alpha_{j1}\mathrm{sinc}(\phi_{j1}t)] \exp(\phi_j t) \tag{13}$$

can be dealt with as follows. When sampling

$$g_k := (k\Delta)f_k = \sum_{j=1}^{n} [\alpha_j k\Delta + (\alpha_{j1}/\phi_{j1})\sin(\phi_{j1}k\Delta)] \exp(\phi_j k\Delta), \qquad k = 0, 1, 2, \ldots$$

the results of the previous subsections can be combined. The formal series with coefficients $g_k, k = 0, 1, 2, \ldots$ is the series development of the sum of the partial fraction decompositions

$$G(z) = \sum_{j=1}^{n} \left(\frac{-\alpha_j \Delta}{1 - \Phi_j z} + \frac{\alpha_j \Delta}{(1 - \Phi_j z)^2} \right) + \sum_{j=1}^{n} \left(\frac{\alpha_{j1}/(2\phi_{j1})}{1 - \Phi_j \Phi_{j1} z} + \frac{-\alpha_{j1}/(2\phi_{j1})}{1 + \Phi_j \Phi_{j1} z} \right)$$

So, every sinc modulated term with exponent ϕ_j translates to four poles in the Padé approximation problem, namely a double pole at $1/\Phi_j$ and two adjacent poles at $\pm(1/\Phi_{j1})(1/\Phi_j)$.

3.4. Frequency modulation

We consider some trigonometric frequency modulation, as in

$$f(t) = \sum_{j=1}^{n} \alpha_j \exp\left(\mathrm{i}(\phi_j t + \alpha_{j1}\sin(\phi_{j1}t))\right), \qquad \alpha_j, \phi_j \in \mathbb{C}, \qquad \alpha_{j1}, \phi_{j1} \in \mathbb{R}. \tag{14}$$

9

Here ϕ_j is often called the carrier frequency and ϕ_{j1} the modulation frequency. Making use of the Jacobi-Anger expansion

$$\exp(\mathrm{i}\alpha\sin\phi) = \sum_{\ell=-\infty}^{+\infty} J_\ell(\alpha)\exp(\mathrm{i}\ell\phi),$$

we can write

$$f(t) = \sum_{j=1}^{n} \alpha_j \left[\sum_{\ell=-\infty}^{+\infty} J_\ell(\alpha_{j1})\exp\left(\mathrm{i}(\phi_j + \ell\phi_{j1})t\right) \right],$$

where $J_\ell(\cdot)$ denotes the Bessel function of the first kind of integer order ℓ. These infinite sums are of course terminated when the terms become negligible, and thus

$$f(t) \approx \sum_{j=1}^{n} \alpha_j \left[\sum_{\ell=-\mu_j}^{+\mu_j} J_\ell(\alpha_{j1})\exp\left(\mathrm{i}(\phi_j + \ell\phi_{j1})t\right) \right].$$

In the same way as in Section 2, the right hand side can be associated with the rational function

$$F(z) = \sum_{j=1}^{n} \sum_{\ell=-\mu_j}^{+\mu_j} \frac{\alpha_j J_\ell(\alpha_{j1})}{1 - \Phi_j \Phi_{j1}^\ell z}, \qquad \Phi_j = \exp(\mathrm{i}\phi_j\Delta), \qquad \Phi_{j1} = \exp(\mathrm{i}\phi_{j1}\Delta)$$

of degree $\mathfrak{n} = n + 2(\mu_1 + \cdots + \mu_n)$ in the denominator and degree $\mathfrak{n} - 1$ in the numerator. The values α_j and α_{j1} can be separated by using

$$\frac{2\ell}{\alpha_{j1}} = \frac{J_{\ell-1}(\alpha_{j1})}{J_\ell(\alpha_{j1})} + \frac{J_{\ell+1}(\alpha_{j1})}{J_\ell(\alpha_{j1})}, \qquad \ell = -\mu_j + 1, \ldots, \mu_j - 1.$$

When one of the $\phi_{j1}, j = 1, \ldots, n$ equals zero, then $\mu_j = 0$ for that ϕ_{j1}. We further assume that all poles are simple and distinct and can be computed using the generalized eigenvalue formulation (4). In practice, the collision of sideband elements $\Phi_j \Phi_{j1}^\ell$ for various j and ℓ, is avoided by engineers [22].

When dealing with distinct $\Phi_j \Phi_{j1}^\ell, j = 1, \ldots, n, \ell = -\mu_j, \ldots, \mu_j$, it is straightforward to group the terms per value of j, in other words to reconstruct model (14) from $F(z)$, by repeating the following steps until the n arithmetical progressions are separated:

1) Organize the frequency estimates in ascending order and calculate the differences of all frequencies with respect to the first one.

2) Extract the first one and the frequencies which are at equidistant intervals of the first one and repeat the steps till all are separated.

10

4. Validation through decimation

4.1. Validated exponential analysis

When replacing Δ by a multiple $\Delta(r) := r\Delta$ and thus sampling at $k\Delta(r) = kr\Delta$, we fill the Hankel matrices $H_n^{(m)}$ with the samples f_{kr} instead of the samples $f_k, k = m, \ldots, m + 2n - 1$. To avoid confusion we denote the latter ones by

$$H_n^{(m)}(r) := \begin{pmatrix} f_{mr} & \cdots & f_{(m+n-1)r} \\ \vdots & \ddots & \vdots \\ f_{(m+n-1)r} & \cdots & f_{(m+2n-2)r} \end{pmatrix}.$$

So the eigenvalues we retrieve from (4) are not $\lambda_j = \Phi_j$, but

$$\lambda_j(r) = \lambda_j^r = \Phi_j^r, \qquad j = 1, \ldots, n.$$

From $\lambda_j^r = \exp(r\phi_j\Delta)$ the imaginary part of ϕ_j cannot be retrieved uniquely anymore, because now

$$|\Im(r\phi_j\Delta)| < r\pi.$$

So aliasing may have kicked in: because of the periodicity of the function $\exp(ir\Im(\phi_j)\Delta)$ a total of r values in the $2r\pi$ wide interval $(-r\pi, r\pi)$ can be identified as plausible values for ϕ_j. Note that when the original λ_j are clustered, the powered λ_j^r may be distributed quite differently and unclustered. Such a
relocation of the generalized eigenvalues can seriously improve the conditioning of the Hankel matrices involved [9].

Remains to investigate how to solve the aliasing problem in the imaginary parts $\Im(\phi_j)$. This aliasing can be fixed at the expense of a small number of additional samples. To fix the aliasing, we add n samples to the $f_0, f_r, \ldots, f_{(2n-1)r}$,
namely at the shifted points $kr\Delta + \rho\Delta$ for $k = h, \ldots, h + n - 1$ with $0 \leq h \leq n$. Easy choices for ρ and r are small mutually prime integer numbers. With the additional samples we proceed as follows.

From the samples $f_0, f_r, \ldots, f_{(2n-1)r}$ we compute the generalized eigenvalues $\lambda_j^r = \exp(\phi_j r\Delta) = \Phi_j^r$ and the coefficients α_j going with Φ_j^r from the linear

system

$$f(kr\Delta) = \sum_{j=1}^{n} \alpha_j \exp(\phi_j kr\Delta) = \sum_{j=1}^{n} \alpha_j \Phi_j^{kr}, \qquad k = 0, \ldots, 2n - 1. \qquad (15)$$

So we know which coefficient α_j goes with which generalized eigenvalue Φ_j^r, but we just cannot identify the correct $\Im(\phi_j)$ from Φ_j^r. The samples at the additional points satisfy

$$
\begin{aligned}
f(kr\Delta + \rho\Delta) &= \sum_{j=1}^{n} \alpha_j \exp\left(\phi_j(kr + \rho)\Delta\right) \\
&= \sum_{j=1}^{n} (\alpha_j \Phi_j^{\rho})\Phi_j^{kr}, \qquad k = h, \ldots, h + n - 1,
\end{aligned}
\qquad (16)
$$

which can be interpreted as a linear system with the same coefficient matrix as (15), but now with a new left hand side and new unknowns $\alpha_1\Phi_1^{\rho}, \ldots, \alpha_n\Phi_n^{\rho}$ instead of $\alpha_1, \ldots, \alpha_n$. And again we can associate each computed $\alpha_j\Phi_j^{\rho}$ with the proper generalized eigenvalue Φ_j^r. Then by dividing the $\alpha_j\Phi_j^{\rho}$ computed from (16) by the α_j computed from (15), for $j = 1, \ldots, n$, we obtain from Φ_j^{ρ} a second set of ρ plausible values for $\Im(\phi_j)$ in the interval $(-\rho\pi, \rho\pi)$. Because of the fact that we choose ρ and r relatively prime, the two sets of plausible values for $\Im(\phi_j)$ have only one value in their intersection [9]. Thus the aliasing problem is solved.

The idea to use or bring in samples at shifted sampling locations can be repeated. Instead of only shifting over ρ, we can choose to repeat the shift over $2\rho, 3\rho, \ldots, (M - 1)\rho$:

$$
\begin{aligned}
f(kr\Delta + m\rho\Delta) &= \sum_{j=1}^{n} \alpha_j \exp\left(\phi_j(kr + m\rho)\Delta\right) \\
&= \sum_{j=1}^{n} (\alpha_j \Phi_j^{m\rho})\Phi_j^{kr}, \qquad k = h, \ldots, h + n - 1, \qquad m = 1, \ldots, M - 1.
\end{aligned}
$$

From each shift over $m\rho$ we compute the coefficients $\alpha_j\Phi_j^{m\rho}$ as in (16), and so for each j we can set up the sequence of values

$$\alpha_j, \alpha_j\Phi_j^{\rho}, \ldots, \alpha_j\Phi_j^{m\rho}, \ldots, \alpha_j\Phi_j^{(M-1)\rho}.$$

With j fixed, these values by themselves follow a one-term exponential model. Therefore we can use a Prony-like method on this sequence of coefficients to

12

extract Φ_j^ρ rather than obtain only one estimate for it from (16). This further stabilizes the estimation of Φ_j^ρ.

The decimation technique can nicely be combined with the Padé view. For a fixed integer $r > 0$ the full sequence of samples $f_0, f_1, f_2, \ldots$ can be divided into r downsampled subsequences

$$f_0, f_r, f_{2r}, \ldots$$
$$f_1, f_{r+1}, f_{2r+1}, \ldots$$
$$\vdots$$
$$f_{r-1}, f_{2r-1}, f_{3r-1}, \ldots$$

where the sequence starting with f_1 can be used as a shift over $\rho = 1$ of the downsampled sequence starting with f_0 and so on. Since we only need n samples at shifted points (and not $2n$), the sequence containing f_r can be used as the shift over $\rho = 1$ of the last subsequence. And of course, shifted sample sequences $f_{kr+\rho}$ for other values of ρ can also be regarded as long as $\gcd(r, \rho) = 1$.

In this way we obtain r smaller problems of the form (15) instead of just one large problem of the form (2), thereby improving the conditoning of the matrices involved. In each of these, assuming that we overshoot the true number of components n in (15) and (16) by $\eta > n$, the true parameters ϕ_j in (1) appear as n stable poles in the Padé approximant while the $\eta - n$ spurious noisy poles behave in an unstable way. In fact, each downsampled sequence can be seen as a different noise realization while the underlying function $f(t)$ remains the same. So the generalized eigenvalues related to the signal $f(t)$ cluster near the true Φ_j^r, and similarly for the Φ_j^ρ associated with the true Φ_j^r, while the other values belong to independent noise realizations and do not form clusters anywhere [23, 24].

The cluster analysis method used in the examples below is DBSCAN [25]. Since the cluster radii may vary, we typically perform at least two runs of DBSCAN with different parameter settings. In a first run we retrieve the clusters with higher density, while subsequent runs allow to detect the less dense clusters

of generalized eigenvalues [10]. We emphasize that the above technique can be combined with any implementation to solve problem (1), or rather (15) and (16), popular methods being described in [26, 27, 6, 28]. The combination of one of these methods with the validation add-on described above, has been termed VEXPA, an acronym for Validated EXPonential Analysis [10]. In the sequel we use the matrix pencil method [6] as the method of choice underlying VEXPA. When including a rank reduction step in matrix pencil, we refer to it as MP-SVD. Its use without rank reduction is simply termed MP.

4.2. Adaptation for modulated signals

When dealing with non-distinct frequencies in the exponential analysis, which translate to poles of higher multiplicity in the Padé approximation problem, as in certain modulated signals, then (5) needs to be replaced by a confluent Vandermonde system, both in the standard as well as in the decimated version (15). We immediately write down the version for a signal decimated by a factor r. Putting $r = 1$ results in the non-decimated case. In (11) the coefficients $\alpha_{j\ell}$ are obtained from

$$
\begin{pmatrix}
1 & 1 & \cdots & 1 & \cdots & 1 & \cdots & 1 \\
\Phi_1^r & \binom{1+r}{1}\Phi_1^r & \cdots & \binom{\mu_1-1+r}{\mu_1-1}\Phi_1^r & \cdots & \Phi_n^r & \cdots & \binom{\mu_n-1+r}{\mu_n-1}\Phi_n^r \\
\vdots & \vdots & & \vdots & & \vdots & & \vdots \\
\Phi_1^{(N-1)r} & \binom{1+(N-1)r}{1}\Phi_1^{(N-1)r} & \cdots & \binom{\mu_1-1+(N-1)r}{\mu_1-1}\Phi_1^{(N-1)r} & \cdots & \Phi_n^{(N-1)r} & \cdots & \binom{\mu_n-1+(N-1)r}{\mu_n-1}\Phi_n^{(N-1)r}
\end{pmatrix}
$$

$$
\times
\begin{pmatrix}
\alpha_{1,0} \\
\vdots \\
\alpha_{1,\mu_1-1} \\
\vdots \\
\alpha_{n,0} \\
\vdots \\
\alpha_{n,\mu_n-1}
\end{pmatrix}
=
\begin{pmatrix}
f_0 \\
f_r \\
\vdots \\
f(N-1)r
\end{pmatrix}. \quad (17)
$$

For the computation of the altered coefficients from the shifted samples in (16), each combinatorial term in (17) containing a multiple $kr, k = 1, \ldots, N - 1$ sees

14

the kr replaced by $kr + \rho$, while the first row of the matrix in (17) becomes

$$1 \quad \binom{1 + \rho}{1} \quad \cdots \quad \binom{\mu_1 - 1 + \rho}{\mu_1 - 1} \quad \cdots \quad 1 \quad \cdots \quad \binom{\mu_n - 1 + \rho}{\mu_n - 1}.$$

The vector of unknowns is now $\left(\alpha_{1,0}\Phi_1^\rho, \cdots, \alpha_{1,\mu_1-1}\Phi_1^\rho, \cdots, \alpha_{n,0}\Phi_n^\rho, \cdots, \alpha_{n,\mu_n-1}\Phi_n^\rho\right)^T$ and the right hand side $\left(f_\rho, f_{r+\rho}, \cdots, f_{(N-1)r+\rho}\right)^T$. Again dividing the solution

$$\left(\alpha_{1,0}\Phi_1^\rho, \cdots, \alpha_{1,\mu_1-1}\Phi_1^\rho, \cdots, \alpha_{n,0}\Phi_n^\rho, \cdots, \alpha_{n,\mu_n-1}\Phi_n^\rho\right)^T$$

componentwise by $\left(\alpha_{1,0}, \cdots, \alpha_{1,\mu_1-1}, \cdots, \alpha_{n,0}, \cdots, \alpha_{n,\mu_n-1}\right)$ gives us estimates for the $\Phi_j^\rho, j = 1, \ldots, n$. From here the validation add-on can proceed as explained above.

5. Examples and numerical illustration

We list some typical computational science and engineering situations in which either the amplitude or the frequency is modulated. For each of the modulation types discussed above, we select an example from the scientific literature and compare with the results obtained there. In these practical applications the matrices in (4) and (5) or (9) and (17) are enlarged to make the problems overdetermined so that they must be solved in a least-squares sense. We therefore introduce the notation

$$H_{\mathbf{n},n}^{(m)} = \begin{pmatrix} f_m & \cdots & f_{m+n-1} \\ \vdots & \ddots & \vdots \\ f_{m+n-1} & \cdots & f_{m+2n-2} \\ \vdots & & \vdots \\ f_{m+\mathbf{n}-1} & \cdots & f_{m+\mathbf{n}+n-2} \end{pmatrix},$$

for the rectangular $\mathbf{n} \times n$ version of the Hankel matrix $H_n^{(m)}$. Usually, the exact sparsity n (or $\mathbf{n}$ in case of modulation) is unknown and consequently overestimated by η, which then becomes the number of columns in the Hankel matrices. The total number of samples needed to construct $H_{\mathbf{n},\eta}^{(0)}$ and $H_{\mathbf{n},\eta}^{(1)}$ is $N = \mathbf{n} + \eta$.

15

All data used in the illustrations are contaminated by noise with a signal-to-noise ratio (SNR) that is typical for the considered application. Our results consistently make use of the validation methods described in Section 4.

5.1. Linear amplitude modulation

Modulation by Laguerre polynomials often occurs in the estimation of time delays [29], for instance in modeling fluorescence decay in biomedical engineering. Signals involving multiple poles in $F(z)$ also appear in the modelling of transverse electromagnetic waves [30] and in modelling the evolution of interest rates in finance [31]. A simple physical example of quadratic amplitude modulation is the critically damped harmonic motion of a spring-mass system [32] which involves a triple pole in $F(z)$.

We construct a linearly modulated example, as a proof of concept of the validation technique. In theory, we then find double poles in $F(z)$, each double pole associated with an exponential term. In practice, due to the presence of noise, we find for every exponential term two close poles. As pointed out in Section 3.1, the poles cannot be retrieved from MP or MP-SVD but should be retrieved from (8). However, since the validation technique retrieves the Φ_j^r and Φ_j^ρ for $j = 1, \ldots, \mathfrak{n}$, the distance between close poles is magnified to the power r and ρ and this can save the computation when using MP or MP-SVD in combination with the validated technique VEXPA. Our example illustrates what can be expected. Consider

$$f(t) = \left(0.1 + 0.2\binom{1 + t/\Delta}{1}\right)\exp(-\mathrm{i}0.04\pi t) + \left(0.3 + 0.15\binom{1 + t/\Delta}{1}\right)\exp(-\mathrm{i}0.06\pi t)$$

with $n = 2, \mathfrak{n} = 4$ and take $\Delta = 1$. We collect 300 samples $f_0, \ldots, f_{299}$ with white Gaussian noise added to achieve a SNR of 20 dB.

When analyzing the signal using the well-known matrix pencil method [6] to solve the least-squares generalized eigenvalue problem

$$H_{200,100}^{(1)} v_j = \lambda_j H_{200,100}^{(0)} v_j,$$

including a reduction of $H_{200,100}^{(0)}$ and $H_{200,100}^{(1)}$ to rank $\mathfrak{n} = 4$ matrices, erroneous results are returned, despite the fact that the correct sparsity $\mathfrak{n}$ is passed. As

16

mentioned in Section 4.1, the use of the matrix pencil method jointly with a
rank reduction step is referred to as the MP-SVD method. The method returns
two close frequencies approximating ϕ_1, a third frequency in the neighbourhood
of ϕ_2 and a fourth frequency that is way off. So for the computation of the
amplitudes $\alpha_{j\ell}, j = 1, 2, \ell = 0, 1$ we have to work with the delivered multiplicities
$\mu_1 = 2, \mu_2 = 1, \mu_3 = 1$ totalling to $\mathfrak{n} = 4$, but with an erroneous value for n in (10).

The validated technique (we choose $r = 4, \rho = 3, M = 1$) is combined with
a rank reduction of the involved Hankel matrices to 8 instead of 4 and is used
on top of this MP-SVD implementation for the solution of each of the r smaller
exponential analysis problems, each of them using only 75 samples instead of
300.

In Table 1 we show the relative errors on the computed values for the double
root ϕ_1 and the amplitudes α_{10}, α_{11} and the double root ϕ_2 and the amplitudes
α_{20}, α_{21}, averaged over 20 runs.

Table 1: Relative errors of linearly modulated signal analysis
(SNR = 20 dB, $N = 300, \mathfrak{n} = 4$).

	MP-SVD	validation
ϕ_1	8.2×10^{-2}	8.7×10^{-3}
ϕ_1	8.2×10^{-2}	8.7×10^{-3}
α_{10}	2.7×10^{2}	3.5×10^{1}
α_{11}	2.1×10^{0}	9.8×10^{-3}
ϕ_2	5.8×10^{-3}	4.9×10^{-3}
ϕ_2	6.7×10^{0}	4.9×10^{-3}
α_{20}	3.5×10^{1}	8.3×10^{0}
α_{21}	2.8×10^{1}	2.9×10^{-2}

5.2. Cosine amplitude modulation

The increase in the use of sensitive nonlinear electronic loads in industrial,
commercial and domestic applications, necessitates a proper understanding of

17

possible power quality disturbances in a distribution system. One of the undesirable effects associated with voltage changes is voltage flicker [33], which is a function of both the frequency and magnitude of the voltage fluctuations. When voltage changes occur in rapid succession with sufficiently large magnitudes, they cause annoying lighting level variations.

Voltage flicker is just one of the power quality disturbances. We use it here as an example because it can be expressed as a trigonometric amplitude modulated waveform. In general, power signal noise results in a SNR of approximately 30 dB. In [33] the authors consider a so-called more complicated voltage flicker given by

$$f(t) = \big[1 + 0.074 \cos(56\pi t) + 0.05 \cos(20\pi t)\big] \cos(100\pi t) +$$
$$0.06 \cos(60\pi t) + 0.05 \cos(178\pi t) + 0.04 \cos(450\pi t).$$

So $n = 8$ and $\mathfrak{n} = 16$ when expressing the signal as an exponential sum. With the frequencies occurring in complex conjugate pairs, we are giving the ones with positive imaginary part odd indices (the ones with negative imaginary part and even indices are not further discussed separately). The noise-free signal is shown in Figure 1.
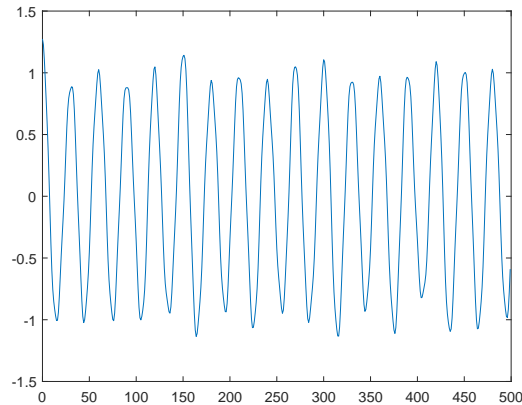

Figure 1: Real-valued voltage flicker $f(k/1500), k = 0, 1, 2, \ldots$

We take $\Delta = 1/1500$, $N = 360$ and add 25 dB white Gaussian noise. Without

18

giving the stand-alone MP method the benefit of a rank reduction of the matrices to $\mathfrak{n} = 16$, and thus revealing the correct sparsity, a typical spectral analysis result looks like in Figure 2 at the left. For the validation we further choose $r = 3, \rho = 1, M = 2$ and compare to the results in [33] which have similar SNR and N. A typical spectral analysis result using VEXPA is shown in Figure 2 at the right. In the latter no rank reduction was performed. So the correct sparsity $\mathfrak{n} = 16$ is (in most of the runs) automatically detected, although we take $\eta = 50$ in each decimated problem using $N/r = 120$ samples. In Table 2 we give a typical relative error for this example.

Table 2: Relative errors of trigonometrically modulated signal analysis
$(\text{SNR}= 25 \text{ dB}, \ N = 360, \mathfrak{n} = 16)$.

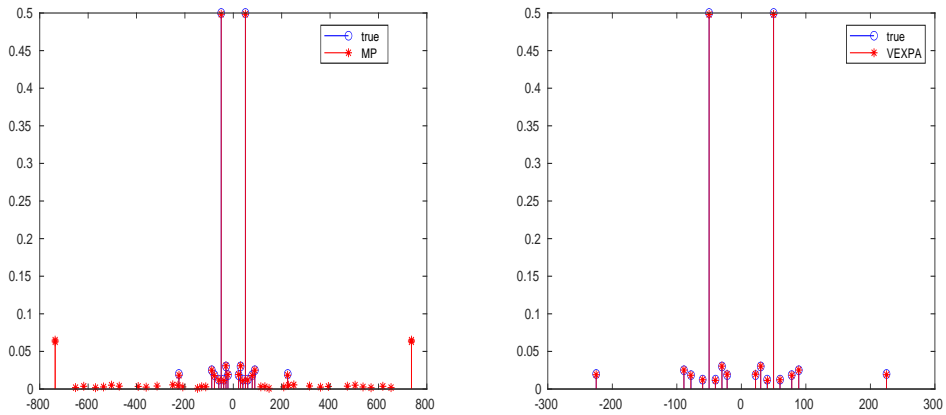|	[33]	new		[33]	new		[33]	new
ϕ_{10}	0.0001	0.0001	$\text{abs}(\alpha_{10})$	0.0031	0.0027	$\arg(\alpha_{10})$	0.0042	0.0055
ϕ_{11}	0.0209	0.0070	$\text{abs}(\alpha_{11})$	0.0486	0.0616	$\arg(\alpha_{11})$	0.2337	0.2984
ϕ_{12}	0.0101	0.0176	$\text{abs}(\alpha_{12})$	0.0020	0.0782	$\arg(\alpha_{12})$	0.1556	0.4362
ϕ_{30}	0.0144	0.0035	$\text{abs}(\alpha_{30})$	0.1333	0.0362	$\arg(\alpha_{30})$	0.2509	0.0719
ϕ_{50}	0.0009	0.0017	$\text{abs}(\alpha_{50})$	0.0260	0.0303	$\arg(\alpha_{50})$	0.1503	0.1339
ϕ_{70}	0.0019	0.0013	$\text{abs}(\alpha_{70})$	0.0375	0.0583	$\arg(\alpha_{70})$	0.3826	0.3960

Figure 2: MP spectral analysis (left, $\eta = 50$) and validated spectral analysis (right, $\eta = 50$).

5.3. Frequency modulation

Micro-motion appears in many situations and causes frequency modulation. Among others, we mention the vibration of a running engine [34], the rotation of a radar antenna on a ship [35], and the like. When a radar transmits an electromagnetic signal to such a target, one observes a micro-Doppler effect due to the micro-motion in addition to the regular Doppler frequency shift due to the target's displacement. The micro-Doppler effect translates to sidebands of the Doppler frequency. The specific type of a moving vehicle can be determined from the micro-Doppler signature of its engine's vibration. Similarly, mechanical oscillations of a bridge or building can be detected in radar returned signals. In most practical micro-Doppler signals the noise cannot be ignored, as its SNR can easily range from 15 dB to 0 dB.

We analyze the weakly modulated micro-Doppler signal given in [36],

$$f(t) = \exp(\mathrm{i}120\pi t + \mathrm{i}0.1\sin(40\pi t)), \tag{18}$$

and take $\Delta = 1/1000, N = 1024, \mathfrak{n} = 682, \eta = 342$. From (18) we know that $n = 1$ and the authors of [36] take $\mu_1 = 1$ so that $\mathfrak{n} = 3$. We add 10 dB white Gaussian noise and perform a reduction of the Hankel matrices to rank 20 matrices, both in the MP-SVD method and the validation technique. Note from Figure 3 that the correct sparsity is hard to deduce from the singular value decomposition of $H_{682,342}^{(0)}$. Nevertheless, the validated technique (with $r = 4, \rho = 1, M = 2$) averagely speaking, returns the correct number $\mathfrak{n} = 3$ of clusters, as can be seen in Figure 4, where we illustrate some average spectral analysis results. From the left figure it is clear that the 3 significant terms cannot be recovered, while the figure at the right leaves no doubt.
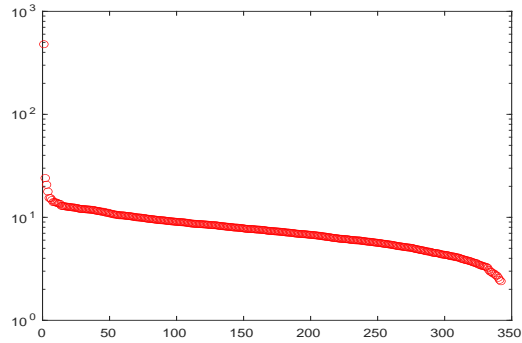
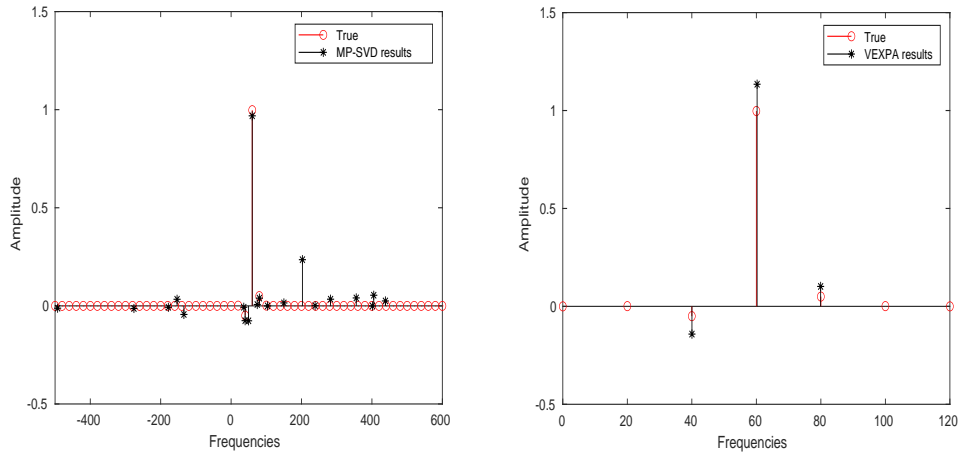Figure 3: Log-plot of singular values of $H_{682,342}^{(0)}$

Figure 4: MP-SVD spectral analysis (left, $\eta = 20$) and validated analysis (right, $\eta = 20$).

6. Conclusion

With non-stationary signals being even more difficult to analyze reliably, the validated exponential analysis add-on plays a significant role. From the many experiments that were carried out, we have shown some typical results on a variety of modulated signals, thereby illustrating the advantage to combine exponential analysis with the proposed alias-free decimation technique which builds on results from Padé approximation theory.

21

References

[1] R. de Prony, Essai expérimental et analytique sur les lois de la dilatabilité des fluides élastiques et sur celles de la force expansive de la vapeur de l'eau et de la vapeur de l'alkool, à différentes températures, J. Ec. Poly. 1 (22) (1795) 24–76.

[2] F. Hildebrand, Introduction to numerical analysis, Mc Graw Hill, New York, 1956.

[3] H. Padé, Sur la représentation approchée d'une fonction par des fractions rationnelles, Ph.D. thesis, Faculté des sciences de Paris (1892).

[4] J. Nuttall, The convergence of Padé approximants of meromorphic functions, J. Math. Anal. Appl. 31 (1970) 147–153. doi:http://dx.doi.org/10.1016/0022-247X(70)90126-5.

[5] C. Pommerenke, Padé approximants and convergence in capacity, J. Math. Anal. Appl. 41 (1973) 775–780. doi:http://dx.doi.org/10.1016/0022-247X(73)90248-5.

[6] Y. Hua, T. K. Sarkar, Matrix pencil method for estimating parameters of exponentially damped/undamped sinusoids in noise, IEEE Trans. Acoust., Speech, Signal Process. 38 (1990) 814–824. doi:http://dx.doi.org/10.1109/29.56027.

[7] J. Basdevant, The Padé approximation and its physical applications, Fortschritte der Physik 20 (5) (1972) 283–331.

[8] J. Gilewicz, M. Pindor, Padé approximants and noise: rational functions, J. Comput. Appl. Math. 105 (1999) 285–297. doi:http://dx.doi.org/10.1016/S0377-0427(99)00041-2.

[9] A. Cuyt, W.-s. Lee, How to get high resolution results from sparse and coarsely sampled data, Appl. Comput. Harmon. Anal. 48 (2020) 1066–1087, (Published online October 11, 2018). `doi:https://doi.org/10.1016/j.`
`acha.2018.10.001.`

[10] M. Briani, A. Cuyt, F. Knaepkens, W.-s. Lee, VEXPA: Validated EXPonential Analysis through regular subsampling, Signal Processing (Published online July 17, 2020).

[11] L. Weiss, R. McDonough, Prony's method, Z-transforms, and Padé approximation, SIAM Rev. 5 (1963) 145–149.

[12] H. Nyquist, Certain topics in telegraph transmission theory, Trans. Am. Inst. Electr. Eng. 47 (2) (1928) 617–644. `doi:http://dx.doi.org/10.`
`1109/T-AIEE.1928.5055024.`

[13] C. E. Shannon, Communication in the presence of noise, Proc. IRE 37 (1949) 10–21.

[14] P. Henrici, Applied and computational complex analysis I, John Wiley & Sons, New York, 1974.

[15] G. Baker, Jr., P. Graves-Morris, Padé approximants (2nd Ed.), Vol. 59 of Encyclopedia of Mathematics and its Applications, Cambridge University Press, 1996.

[16] E. Kaltofen, W.-s. Lee, Early termination in sparse interpolation algorithms, J. Symbolic Comput. 36 (3-4) (2003) 365–400, international Symposium on Symbolic and Algebraic Computation (ISSAC 2002) (Lille). `doi:http://dx.doi.org/10.1016/S0747-7171(03)00088-9.`

[17] J. Gammel, Effect of random errors (noise) in the terms of a power series on the convergence of the Padé approximants, in: P. Graves-Morris (Ed.), Padé approximants, 1972, pp. 132–133.

23

[18] J. Gilewicz, M. Pindor, Padé approximants and noise: a case of geometric series, J. Comput. Appl. Math. 87 (1997) 199–214. `doi:http://dx.doi.org/10.1016/S0377-0427(97)00185-4`.

[19] A. Sidi, Interpolation at equidistant points by a sum of exponential functions, J. Approx. Theory 34 (1982) 194–210.

[20] K. Stampfer, G. Plonka, The generalized operator based Prony method, Constr. Approx.`doi:https://doi.org/10.1007/s00365-020-09501-6`.

[21] A. Cuyt, W.-s. Lee, Parametric spectral analysis: scale and shift, ArXiv e-print 2008.02125 [cs.NA], Universiteit Antwerpen (2020).

[22] Z. Wang, Z. He, C. Gao, A systematic study on the harmonic overlap effects for DC/AC converters under low switching frequency modulation, Energies 14 (10) (2021) 2811.

[23] P. Barone, On the distribution of poles of Padé approximants to the Z-transform of complex Gaussian white noise, Journal of Approximation Theory 132 (2) (2005) 224 – 240. `doi:http://dx.doi.org/10.1016/j.jat.2004.10.014`.

[24] L. Perotti, T. Regimbau, D. Vrinceanu, D. Bessis, Identification of gravitational-wave bursts in high noise using Padé filtering, Phys. Rev. D 90 (2014) 124047. `doi:https://dx.doi.org/10.1103/PhysRevD.90.124047`.

[25] M. Ester, H.-P. Kriegel, J. Sander, X. Xu, A density-based algorithm for discovering clusters a density- based algorithm for discovering clusters in large spatial databases with noise, in: Proceedings of the Second International Conference on Knowledge Discovery and Data Mining, KDD'96, AAAI Press, 1996, pp. 226–231.

[26] R. Schmidt, Multiple emitter location and signal parameter estimation, IEEE Trans. Antennas Propag. 34 (3) (1986) 276–280. `doi:http://dx.doi.org/10.1109/TAP.1986.1143830`.

[27] R. Roy, T. Kailath, ESPRIT-estimation of signal parameters via rotational invariance techniques, IEEE Trans. Acoust., Speech, Signal Process. 37 (7) (1989) 984–995. `doi:http://dx.doi.org/10.1109/29.32276`.

[28] W. M. Steedly, C.-H. J. Ying, R. L. Moses, Statistical analysis of TLS-based Prony techniques, Automatica J. IFAC 30 (1) (1994) 115–129. `doi: https://dx.doi.org/10.1016/0005-1098(94)90232-1`.

[29] A. Sabatini, Correlation receivers using Laguerre filter banks for modelling narrowband ultrasonic echoes and estimating their time-of-flights, IEEE Trans. Ultrason., Ferroelectr., Freq. Control. 44 (6) (1997) 1253–1263. `doi: 10.1109/58.656629`.

[30] P. Milonni, J. Eberly, Lasers, John Wiley & Sons, New York, 1988.

[31] D. Filipović, Exponential-polynomial families and the term structure of interest rates, Bernoulli (2000) 1081–1107.

[32] R. Badeau, G. Richard, B. David, Performance of ESPRIT for estimating mixtures of complex exponentials modulated by polynomials, IEEE Trans. Signal Process. 56 (2) (2008) 492–504. `doi:10.1109/TSP.2007.906744`.

[33] C.-I. Chen, Y.-C. Chen, Y.-R. Chang, Y.-D. Lee, An accurate solution procedure for calculation of voltage flicker components, IEEE Trans. Ind. Electron. 61 (5) (2014) 2370–2377. `doi:10.1109/TIE.2013.2270221`.

[34] V. Chen, F. Li, S.-S. Ho, H. Wechsler, Micro-Doppler effect in radar: phenomenon, model, and simulation study, IEEE Trans. Aerosp. Electron. Syst. 42 (1) (2006) 2–21. `doi:10.1109/TAES.2006.1603402`.

[35] C. Cai, W. Liu, J. Fu, L. Lu, Empirical mode decomposition of micro-Doppler signature, in: IEEE International Radar Conference, IEEE, 2005, pp. 895–899. `doi:10.1109/RADAR.2005.1435954`.

[36] Y. Wang, X. Wu, W. Li, Z. Li, Y. Zhang, J. Zhou, Analysis of micro-Doppler signatures of vibration targets using EMD and SPWVD, Neurocomputing 171 (2016) 48–56.